Article

Surface-Assisted Assembly of an Ionic-Complementary Peptide: Controllable Growth of Nanofibers

Hong Yang, Shan-Yu Fung, Mark Pritzker, and P. Chen

J. Am. Chem. Soc., **2007**, 129 (40), 12200-12210• DOI: 10.1021/ja073168u • Publication Date (Web): 13 September 2007

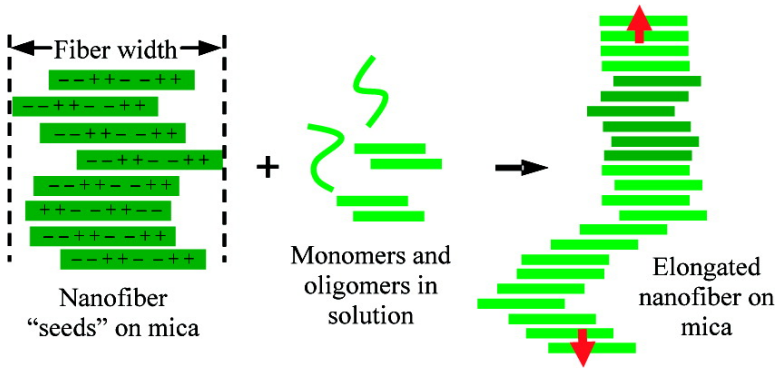

More About This Article

Additional resources and features associated with this article are available within the HTML version:

- Supporting Information
- Links to the 4 articles that cite this article, as of the time of this article download
- Access to high resolution figures
- Links to articles and content related to this article
- Copyright permission to reproduce figures and/or text from this article

View the Full Text HTML

J|A|C|S
ARTICLES
Published on Web 09/13/2007

Surface-Assisted Assembly of an Ionic-Complementary Peptide: Controllable Growth of Nanofibers

Hong Yang, Shan-Yu Fung, Mark Pritzker, and P. Chen*

Contribution from the Department of Chemical Engineering, University of Waterloo, 200 University Avenue West, Waterloo, Ontario N2L 3G1, Canada

Received May 4, 2007; E-mail: p4chen@cape.uwaterloo.ca

Abstract: Numerous studies have shown that a surface can direct and regulate molecular assembly. In this study, the nanofiber growth of an ionic-complementary peptide, EAK16-II, on a mica surface was investigated under various solution conditions via in situ atomic force microscopy. In comparison to the assembly in bulk solution, nanofiber growth of EAK16-II on mica is surface-assisted and involves two steps: (1) adsorption of nanofibers and fiber clusters (from the bulk solution) on the surface, serving as the "seeds"; (2) fiber elongation of the "seeds" from their active ends. The nanofiber growth can be controlled by adjusting the solution pH since it modulates the adsorption of the "seeds" on mica and their growth rates. The amount of the adsorbed "seeds" decreases with increasing solution pH, while the growth rate under different solution conditions is found to follow the order pure water > 1 mM HCl > 1 mM NaOH > 10 mM HCl $\approx$ 10 mM NaOH $\approx$ 0. The pH-dependent nanofiber growth is due to the surface charge of the peptides and peptide assemblies in various solutions as indicated by ζ-potential measurements. A simple model was proposed to describe surface-assisted nanofiber growth. This study provides insights into the assembly of peptide/protein on a surface, which is essential to understand such physiological protein aggregation systems as amyloid fibrillogenesis. In addition, the potential of this finding to construct biocompatible electrodes for biomolecular sensing is also discussed.

1. Introduction

Molecular assembly at a surface plays an important role in many nanotechnology and biological applications.[1−3] Surface/substrate-directed assembly has been explored to construct a variety of nanosystems. For example, a hydrophobic graphite surface was reported to direct molecules, such as long alkyl chains, fullerene derivatives,[4] peptides,[5−7] and polymers,[8] to organize into various patterns. The resulting nanostructures can be used to construct nanoscopic devices, such as (bio)sensors, information storage units, optical computers, and solar cells.[9−12] Another example is the spontaneous organization of the negatively charged virus M13 into ordered monolayer structures on the surface of a positively charged, multilayered LPEI/PAA polymer film.[13] These ordered, self-assembled viral structures can be used to fabricate more powerful batteries and grow functional nanoparticles and nanowires.[13,14]

In biomedical studies, some surfaces have been found to induce protein/peptide aggregation. Recent reports have shown the importance of substrates in amyloid fibril formation.[7,15−17] The size and shape of amyloid-β (Aβ) peptide aggregates, as well as the kinetics of aggregation, exhibited pronounced dependence on the physicochemical properties of the substrate.[7,15,18] The fibrillization of α-synuclein, a protein associated with Parkinson's disease, has been found to depend on the nature of the micelle surface in incubation solution.[17] It was reported that the in vitro fibril formation of some proteins, such as SMA, a recombinant amyloidogenic light chain variable domain, is sensitive to the contact surface of test tube materials and a stir bar.[16] All these observations point to a notion that the substrate effect on protein/peptide assembly and aggregation is important and critical to many nanoscale biomedical processes.

(1) Tirrell, M.; Kokkoli, E.; Biesalski, M. *Surf. Sci.* **2002**, *500*, 61−83.
(2) Lowe, C. R. *Curr. Opin. Struct. Biol.* **2000**, *10*, 428−434.
(3) Malmsten, M. *Biopolymers at Interfaces*, 2nd ed.; Marcel Dekker, Inc.: New York, 2003.
(4) Nakanishi, T.; Miyashita, N.; Michinobu, T.; Wakayama, Y.; Tsuruoka, T.; Ariga, K.; Kurth, D. G. *J. Am. Chem. Soc.* **2006**, *128*, 6328−6329.
(5) Brown, C. L.; Aksay, I. A.; Saville, D. A.; Hecht, M. H. *J. Am. Chem. Soc.* **2002**, *124*, 6846−6848.
(6) Yang, G.; Woodhouse, K. A.; Yip, C. M. *J. Am. Chem. Soc.* **2002**, *124*, 10648−10649.
(7) Kowalewski, T.; Holtzman, D. M. *Proc. Natl. Acad. Sci. U.S.A.* **1999**, *96*, 3688−3693.
(8) Severin, N.; Okhapkin, I. M.; Khokhlov, A. R.; Rabe, J. P. *Nano Lett.* **2006**, *6*, 1018−1022.
(9) Wouters, D.; Schubert, U. S. *Angew. Chem., Int. Ed.* **2004**, *43*, 2480−2495.
(10) Paquim, A. C.; Oretskaya, T. S.; Brett, A. M. O. *Electrochim. Acta* **2006**, *51*, 5037−5045.
(11) Wei, Y.; Tong, W.; Wise, C.; Wei, X.; Armbrust, K.; Zimmt, M. *J. Am. Chem. Soc.* **2006**, *128*, 13362−13363.
(12) Lim, H. S.; Han, J. T.; Kwak, D.; Jin, M.; Cho, K. *J. Am. Chem. Soc.* **2006**, *128*, 14458−14459.
(13) Yoo, P. J.; Nam, K. T.; Qi, J.; Lee, S.; Park, J.; Belcher, A. M. *Nat. Mater.* **2006**, *5*, 234−240.
(14) Nam, K. T.; Kim, D.-W.; Yoo, P. J.; Chiang, C.-Y.; Meethong, N.; Hammond, P. T.; Chiang, Y.-M.; Belcher, A. M. *Science* **2006**, *312*, 885−888.
(15) Ban, T.; Hoshino, M.; Takahashi, S.; Hamada, D.; Hasegawa, K.; Naiki, H.; Goto, Y. *J. Mol. Biol.* **2004**, *344*, 757−767.
(16) Zhu, M.; Souillac, P. O.; Ionescu-Zanetti, C.; Carter, S. A.; Fink, A. L. *J. Biol. Chem.* **2002**, *277*, 50914−50922.
(17) Hoyer, W.; Cherny, D.; Subramaniam, V.; Jovin, T. M. *J. Mol. Biol.* **2004**, *340*, 127−139.
(18) Blackley, H. K. L.; Sanders, G. H. W.; Davies, M. C.; Roberts, C. J.; Tendler, S. J. B.; Wilkinson, M. J. *J. Mol. Biol.* **2000**, *298*, 883−840.

10.1021/ja073168u CCC: $37.00

Scheme 1. Molecular Structure of EAK16-II

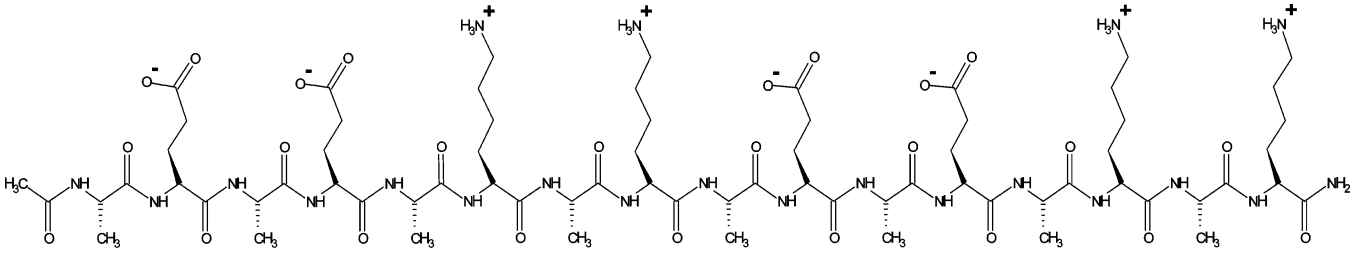

AcN-AEAEAKAKAEAEAKAK-CNH_2

Our understanding of the substrate-assisted assembly and aggregation of biomolecules, however, remains incomplete. This is partially due to the complexity of biomolecules and the experimental difficulties in nanoscale in situ examination of the assemblies. A relatively simple, self-assembling peptide with residues that possess a variety of molecular interactions occurring in proteins could be a good model molecule to investigate such complicated processes. The purpose of this work is thus to study the substrate/surface effects on the nanoassembly of a model peptide, to better understand the assembly kinetics and further to control the peptide aggregation at a surface.

The model peptide used is an ionic-complementary, self-assembling peptide, EAK16-II (Scheme 1).[19−21] This peptide is capable of hydrogen bonding and electrostatic and hydrophobic interactions. The amino acid sequence of this peptide bears a repetitive, alternating charge distribution (type II: − − + + − − + +) leading to ionic complementarity.[19,22] In addition, alternation of the hydrophobic (A, alanine) and hydrophilic (E, glutamic acid, and K, lysine) residues results in an amphiphilic feature. Such an amino acid sequence allows the peptide to self-assemble into β-sheet-rich nanofibers in solution.[19−22] Our previous studies have shown that many factors, such as peptide sequence[20,23] and concentration,[21,24] salt type and concentration,[24−26] and solution pH,[20] affect the self-assembled micro-/nanostructures of the peptide and its derivatives. The simple, regular structure and our previous knowledge of EAK16-II provide a good basis to study the substrate/surface effect on the peptide aggregation and to possibly control this process.

The main tool used was in situ atomic force microscopy (AFM). This technique is especially suitable for real-time monitoring of the assembly of biomolecules in solution. First, this method enables the repetitive imaging of mechanically delicate biomaterials with minimum lateral forces between the probe and sample. Second, it is possible to directly study the dynamics and kinetics of the assembly of proteins/peptides under the solution conditions appropriate for biological events.[27] Third, the kinetics of each individual assembly can be quantified. The surface used in this study was mica, which is negatively charged even at a low pH value of 3[28] and provides an atomically flat surface that enables high-resolution AFM imaging. To complement the AFM surface observations, dynamic light scattering (DLS) and ζ-potential measurements were employed to monitor the assembly process and the charge of the peptide in bulk solution, respectively. It is known that the surface charge of a particle plays an important role in aggregation of colloidal dispersions, polyelectrolytes, and proteins.[29,30] These solution properties of EAK16-II should provide essential information and evidence in relation to surface-assisted assembly.

We in particular investigated the surface-assisted EAK16-II assembly at different solution pHs. It is expected that a change of the solution pH alters the charge status of the peptide and its electrostatic interaction, which in turn should affect the peptide−peptide and peptide−surface interactions. As a result, the assembly behavior of EAK16-II on the substrate may be modified. This will provide a way to control the surface-assisted assembly, leading to construction of functional nanostructures. We will relate our findings to amyloid fibrillogenesis and show a potential exciting application of the peptide assembly in biomolecular sensing.

2. Materials and Methods

2.1. Materials. The peptide EAK16-II ($C_{70}H_{121}N_{21}O_{25}$, molecular weight 1657 g/mol) has a sequence of AEAEAKAKAEAEAKAK (Scheme 1), where A corresponds to alanine, E to glutamic acid, and K to lysine. At neutral pH, A is a neutral, hydrophobic residue, while E and K are negatively and positively charged, respectively. This peptide was purchased from CanPeptide Inc. (Québec, Canada) with a purity of >95% (purified by reversed-phase high-performance liquid chromatography). The N-terminus and C-terminus of the peptide were protected by acetyl and amino groups, respectively, to minimize end-to-end electrostatic interaction between peptides.[23]

The EAK16-II stock solutions were prepared in pure water (18.2 MΩ; Millipore Milli-Q system) at concentrations of 12 and 120 μM and stored at 4 °C before use. Unless otherwise noted, the 12 μM peptide stock solution was used for all AFM studies, whereas the 120 μM peptide stock solution was for transmission electron microscopy (TEM) imaging. Reagent grade sodium hydroxide with purity of 99+% and hydrochloric acid (36−38% by weight) were obtained from BDH Chemicals Ltd. (Toronto, Canada) and Fisher Scientific, Inc. (Nepean, Canada), respectively.

(19) Zhang, S.; Holmes, T.; Lockshin, C.; Rich, A. *Proc. Natl. Acad. Sci. U.S.A.* **1993**, *90*, 3334−3338.
(20) Hong, Y.; Legge, R. L.; Zhang, S.; Chen, P. *Biomacromolecules* **2003**, *4*, 1433−1442.
(21) Fung, S. Y.; Keyes, C.; Duhamel, J.; Chen, P. *Biophys. J.* **2003**, *85*, 537−548.
(22) Zhang, S.; Lockshin, C.; Cook, R.; Rich, A. *Biopolymers* **1994**, *34*, 663−672.
(23) Jun, S.; Hong, Y.; Immamura, H.; Ha, B.-Y.; Bechhoefer, J.; Chen, P. *Biophys. J.* **2004**, *87*, 1249−1259.
(24) Hong, Y.; Lau, L. S.; Legge, R. L.; Chen, P. *J. Adhesion* **2004**, *80*, 913−931.
(25) Hong, Y.; Pritzker, M. D.; Legge, R. L.; Chen, P. *Colloids Surf., B* **2005**, *46*, 152−161.
(26) Yang, H.; Pritzker, M.; Fung, S. Y.; Sheng, Y.; Wang, W.; Chen, P. *Langmuir* **2006**, *22*, 8553−8562.
(27) Santos, N. C.; Castanho, M. A. R. B. *Biophys. Chem.* **2004**, *107*, 133−149.
(28) Nishimura, S.; Scales, P. J.; Tateyama, H.; Tsunematsu, K.; Healy, T. W. *Langmuir* **1995**, *11*, 291−295.
(29) Sato, T.; Ruch, R. *Stabilization of Colloidal Dispersions by Polymer Adsorption*; Marcel Dekker, Inc.: New York, 1980.
(30) Blank, M. *Colloids Surf.* **1989**, *42*, 355−364.

Table 1. Effect of pH of 100 μL of 12 μM EAK16-II Obtained by Preparation in Pure Water and Then Addition to Various Solutions on Fibril Growth on Mica

solution conditions	final pH	fibril deposited on mica	fibril growth on mica	average growth rate (nm/s)
EAK16-II in 10 mM HCl	2.2	yes	no	0
EAK16-II in 1 mM HCl	3.4	yes	yes	0.17 ± 0.10
EAK16-II in pure water	5.0	yes	yes	0.74 ± 0.40
EAK16-II in 1 mM NaOH	9.9	yes	yes	0.008 ± 0.003
EAK16-II in 10 mM NaOH	11.5	yes	no	0

Grade V-4 muscovite mica ($KAl_2(AlSi_3)O_{10}(OH)_2$, SPI Supplies, West Chester, PA) was used as the supporting surface. A mica slide was fixed on an AFM sample plate using a double-sided tape. An adhesive tape was used to remove the outer layer of mica to generate a fresh surface prior to each experiment.

2.2. In Situ AFM Imaging. To monitor how a single EAK16-II nanofiber assembles on a mica surface under desired experimental conditions and avoid any drying effects, in situ AFM imaging was performed on a PicoScan AFM (Molecular Imaging, Phoenix, AZ) in a liquid cell (custom-made). The cell was mounted on a freshly cleaved mica surface and injected with 500 μL of pure water, 1 mM HCl, 10 mM HCl, 1 mM NaOH, or 10 mM NaOH solution. A volume of 100 μL of the 12 μM EAK16-II stock solution was then injected into the liquid cell with a microsyringe to obtain a final peptide concentration of 2 μM. This slightly diluted the concentrations of HCl and NaOH solutions (0.83 and 8.33 mM); however, the same initial concentrations (1 and 10 mM of HCl or NaOH solutions) before the injection of the peptide solution were used throughout this study. The pH values of the final solutions in the liquid cell are indicated in Table 1.

Atomic force microscopy images were obtained using a scanner with a maximum scan area of 6×6 μm^2. All AFM experiments were conducted in an environmentally controlled chamber at room temperature to avoid evaporation of the working solution. Silicon nitride cantilevers with a nominal spring constant of 0.58 N/m (DNP-S, Veeco Probes, Santa Barbara, CA) and a typical tip radius of 10 nm were used in AFM tapping mode. To obtain the best imaging quality, the typical tapping frequency was set between 16 and 18 kHz and the scan rates were controlled between 0.8 and 1 Hz ($\sim$5 min to take each AFM image). All AFM images were collected at a resolution of 256×256 pixels. In general, the elapsed time associated with each image refers to the point when EAK16-II stock solution was injected into the liquid cell containing a desired working solution. An initial image of a newly cleaved mica surface immersed in the working solution was taken to confirm the absence of contaminating dust particles.

The lengths of EAK16-II fibers on the mica surface at different times were measured with the Image J software (http://rsb.info.nih.gov/ij/). The width and height of EAK16-II nanofibers were determined by the cross section analysis tool of the PicoScan software (Molecular Imaging, Phoenix, AZ). The peptide fiber widths reported were obtained using the deconvolution method reported by Fung et al.[21] For each solution condition, at least 50 nanofibers were collected and analyzed from the AFM images of at least three independent experiments.

2.3. TEM Imaging. Transmission electron microscopy was performed with a Philips CM20 electron microscope (Philips Electronics Ltd. Guildford, U.K.) at an accelerating voltage of 200 kV. Images were digitalized using a Gatan 679 slow-scan CCD camera and analyzed using DIGITALMICROGRAPH (version 2.1, Gatan Inc. Pleasanton, CA). A 120 μM EAK16-II stock solution was diluted with pure water 5 times first, and then 10 μL of the diluted solution was incubated on a 400-mesh carbon-coated Formvar copper grid (Marivac Ltd., St. Laurent, QC) for 10 min. Excess solution was drawn off the edge of the grid with tissue paper. After air drying for 20 min, the grid was negatively stained with 2% (w/v) uranyl acetate for 5 s. Excess stains were drawn off with tissue paper, and the grid was air-dried before TEM imaging.

2.4. Dynamic Light Scattering. Dynamic light scattering experiments were performed using a Zetasizer Nano ZS (Malvern Instruments, Worcestershire, U.K.) with the appropriate viscosity and refractive index settings and the temperature maintained at 25 °C during the measurement. A small-volume (45 μL) black quartz cuvette with a 3 mm light path was used. A 0.3 mM EAK16-II solution was prepared in pure water, 1 mM HCl, 10 mM HCl, or 10 mM NaOH and sonicated for 10 min and then filtered (0.22 μm) before the measurement was taken. The scattered light intensities of samples at the angle of 173° were collected at various times. The pH of 0.3 mM EAK16-II dissolved in pure water, 1 mM HCl, 10 mM HCl, and 10 mM NaOH was measured to be 3.9, 3.1, 2.0, and 11.9, respectively. The viscosity and refractive index of pure water, 1 mM HCl, 10 mM HCl, and 10 mM NaOH at 25 °C were also measured by a Cannon Ubbelohde Semi-Micro viscometer (size 75, Cannon Instrument Company, State College, PA) and refractometer (Bausch & Lomb, Inc., Rochester, NY), respectively, and found to be very close to those of pure water at 25 °C.

Under each condition, two samples were used and triplicate measurements were made for each sample. The sample was monitored frequently within the first day, twice a day for the following 4 days, and once every 2 or 3 days for the following 3 weeks. The intensity-based size distribution of peptide assemblies in solution was obtained with the multimodal algorithm CONTIN,[31] provided in the software package Dispersion Technology Software 5.0 (Malvern Instruments, Worcestershire, U.K.).

To study the kinetics of peptide assembly in solution, the total light intensity of the peptide solution was monitored over time. The light intensities reported as a function of time were the average values obtained from three measurements of each sample. The light intensity of the peptide dissolved in pure water was plotted versus time and fitted to a single-exponential function:

$$I(t) = I_{eq} + A \exp(-k_{app}t) \quad (1)$$

where $I(t)$ is the light intensity at time t, I_{eq} is the maximum light intensity at the end of the observed exponential phase, A is the pre-exponential coefficient, and k_{app} is the apparent rate constant.

2.5. ζ-Potential Measurements. The surface charge of EAK16-II assemblies in solution was determined by ζ-potential measurements on a Zetasizer Nano ZS (Malvern Instruments, Worcestershire, U.K.) at 25 °C. Of particular interest is the effect of pH on the ζ-potential of these assemblies. A freshly prepared 0.18 mM EAK16-II solution was used for each measurement. The pH of the peptide solution was adjusted to the desired value using small amounts of 2 M NaOH or 2 M HCl. A correction of the peptide concentration for the volume change was not made for this measurement because the change in peptide concentration (<1%) due to the addition of NaOH or HCl was negligible. Samples were injected into a disposable cell (folded capillary DTS-1060 from Malvern, Worcestershire, U.K.) with a volume of $\sim$1 mL and analyzed at constant voltage. The ζ-potential distribution (in mV) was automatically calculated from the electrophoretic mobility distribution based on the Smoluchowski formula.[32,33] For each solution condition, the ζ-potentials were repeated with two independent samples; at least three measurements were carried out for each sample. The ζ-potentials reported herein correspond to the average of the peak values of the ζ-potential distributions from the repeated measurements.

3. Results

3.1. Real-Time Observation of EAK16-II Nanofiber Growth on Mica. Figure 1a−d shows a sequence of the in situ AFM images of EAK16-II nanofibers taken on the same location of

(31) Provencher, S. W. *Comput. Phys. Commun.* **1982**, *27*, 213.
(32) Adamson, A. W.; Gast, A. P. *Physical Chemistry of Surfaces*, 6th ed.; John Wiley & Sons: New York, 1997.
(33) Evans, D. F.; Wennerstrom, H. *The Colloidal Domain: Where Physics, Chemistry, Biology, and Technology Meet*; VCH Publishers, Inc.: New York, 1994.

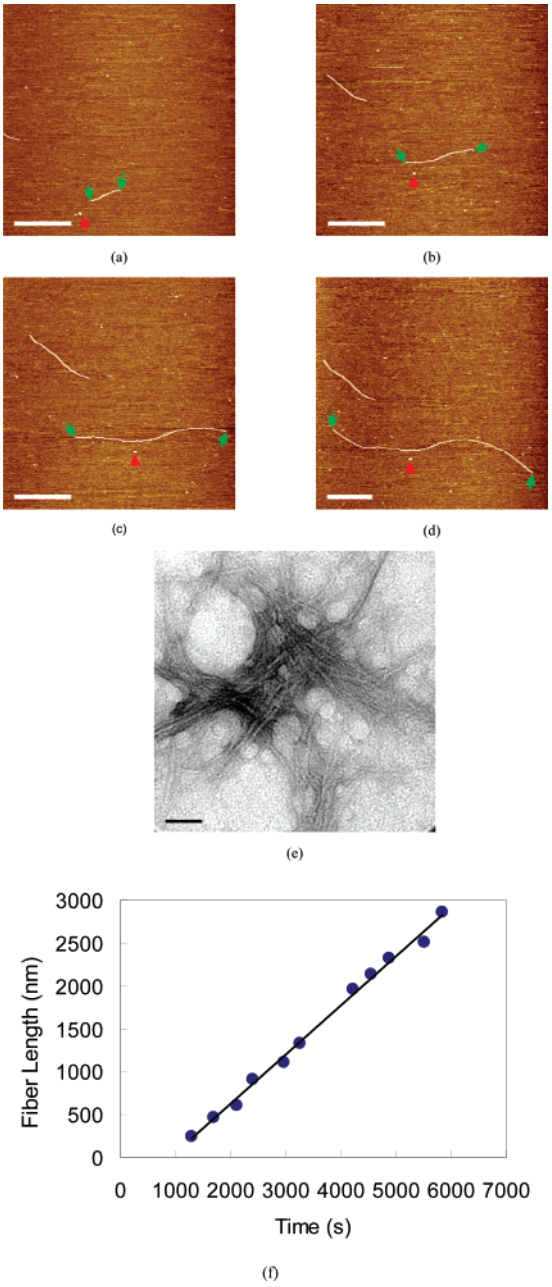

Figure 1. Time evolution of EAK16-II nanofiber growth on a mica substrate in pure water at (a) 1285, (b) 2107, (c) 3251, and (d) 4874 s. Time zero is when peptide solution is added into the AFM liquid cell. The scale bar represents 500 nm. The green arrows point at two ends of a fiber, and the red arrow points at a small globule serving as a reference location on mica. (e) TEM image of EAK16-II self-assembled nanofibers. The scale bar represents 50 nm. (f) Variation of EAK16-II nanofiber length on mica with time.

a mica substrate immersed in an aqueous solution containing 2 μM EAK16-II. It can be seen that the length of nanofibers increases with time. A couple of short nanofibers (~200 nm in length) initially appearing after ~21 min of incubation (Figure 1a) are observed to continually grow on mica (Figure 1b−d). After ~81 min, the nanofiber length increases to ~2.3 μm. The green arrows indicate the two ends of a fiber, while the red arrow points to a reference spot to show that the nanofiber can grow at both ends (bidirectional growth). The elongation from the two ends of a fiber may result from the addition of peptide monomers or oligomers at the two active ends. At this stage, we cannot distinguish whether a monomeric or oligomeric addition is occurring.

From the AFM images, the width and height of newly grown part of fibers on the surface are similar to those of the nanofiber "seeds", which are presumably formed in solution. This suggests that nanofibers formed in bulk solution and on the surface are similar. The width and height of these nanofibers are ~7 nm (after tip deconvolution) and ~1.5 nm, respectively. Since the fiber width measured by AFM is usually affected by the AFM tip,[21] the fiber width was also examined by TEM for comparison (Figure 1e). The TEM image shows that a single EAK16-II nanofiber has a width of ~5 nm, which compares well with the AFM results. The uniform fiber width and height may indicate a special arrangement of peptide molecules in the nanofiber and a possible fiber growth mechanism, as will be discussed later.

The uniform width of nanofibers enables precise analysis of the growth rate of an individual fiber length. Figure 1f shows a plot of the variation of the peptide fiber length (measured between two green arrows) with time. The length of the fiber monitored in Figure 1a−d increases linearly with the incubation time at a rate of 0.57 nm/s over the experiment. The lengths of other fibers also show a predominant linear growth although the growth rates vary from one nanofiber to another. This may be due to the (minute) differences in the fiber characteristics and/or the change of the local environments. It is also worth noting that the growth rate in our study may represent the initial growth state since the time period of in situ AFM imaging is usually less than 2 h. In some cases, the active ends of a growing fiber can be terminated when they encounter other fibers or other small surface features (dots or globules in the AFM image). This will lead to fiber network formation on the mica surface. These small surface features may be peptide globular aggregates or some other components in solution (e.g., impurities). The presence of some globules/small dots throughout all AFM images is reasonable since EAK16-II has been shown to form both globules and fibers especially when the peptide concentration is very low.[23] However, unlike the nanofibers, these globules and small dots do not grow on the surface. If one active end is blocked, the nanofiber can grow from the other end; such a growth pattern can be termed unidirectional fiber growth.

From the analysis of at least 50 independent, growing nanofibers with two active ends on mica, an average growth rate of 0.74 ± 0.40 nm/s is obtained. The observed linear growth of nanofibers might indicate that the fiber elongation occurs by the addition of peptide monomers to the active ends. To relate this growth rate to the number of monomers added, the width of the β-strand EAK16-II molecule was estimated using ChemSketch software (Toronto, Canada). This software determined the width to be 0.3−0.5 nm from the distance between the topmost and bottommost atoms in the van der Waals-based structure (i.e., direction in and out of the plane of the structure shown in Scheme 1). Thus, the observed growth rate corresponds to the attachment of one or two monomers to the active ends of a nanofiber "seed" every second by presuming that the arrangement of peptides in the nanofiber follows a cross-β fashion (see section 4.2).

The increase in the fiber length as a function of time can be described by the following linear relation, within our AFM observation period:

$$\begin{cases} t < \tau_0, l = l_0 \\ t \geq \tau_0, l = l_0 + (t - \tau_0)v \end{cases} \quad (2)$$

where l is the fiber length at time t; l_0 is the length of a nanofiber "seed"; τ_0 is the time when a nanofiber "seed" deposits on mica; v is the fiber growth rate on mica. Although each nanofiber has a different growth rate, one can use an average growth rate at the same solution condition to estimate the length of the nanofiber on the surface at a given time with these equations. One can also estimate the deposition time τ_0 of a "seed" by monitoring its growth rate. For instance, if the length of a nanofiber "seed" is known (e.g., $l_0 \sim 54.6$ nm in 12 μM peptide stock solution, obtained from the statistical analysis of nanofiber length in 10 mM HCl; see section 3.2), τ_0 for "seed" deposition (Figure 1) is estimated to be ~918 s for a fiber that has a growth rate of 0.57 nm/s ($l = 2855.9$ nm at $t = 5833$ s).

The assemblies in self-assembly systems are typically polydispersed with various sizes.[34−36] As will be shown in section 3.3, we also observed this behavior for EAK16-II dissolved in solution. A manifestation of this polydispersity is the formation of large peptide aggregates as fiber clusters on the mica surface, as shown in Figure 2. Over time, many nanofibers begin to grow from these fiber clusters (Figure 2a−d). This suggests that the large aggregates consist of nanofiber bundles/entanglements and the active ends of these fibers on the outer edges of the fiber clusters can continue to grow radially outward.

In order to investigate the rate at which these nanofibers grow from the clusters, the area covered by the fiber clusters on the mica substrate has been analyzed and plotted as a function of time in Figure 2e. It can be seen that the area covered by the fiber clusters also increases linearly with time. Since the nanofiber width remains uniform, the area increases linearly due to a linear increase of the nanofiber length. This suggests that the nanofiber growth from the fiber clusters is similar to that from the single nanofiber "seeds" except that each nanofiber in the former case grows at one end, whereas it can grow at both ends in the latter. The equivalent growth rate of nanofibers from the fiber clusters is determined to be 3.21 nm/s by dividing the area of peptide aggregates by the width of nanofibers (15.6 nm prior to deconvolution). This value is almost 4 times higher than that of the average bidirectional growth rate of nanofibers (0.74 ± 0.40 nm/s). The much faster growth rate of nanofibers from the fiber clusters may be due to the peptide concentration being locally higher around the fiber clusters.

3.2. Effect of Solution pH on EAK16-II Nanofiber Growth on Mica. EAK16-II is ionic-complementary and contains four positively charged residues (K, pK_a of 10.54) and four negatively charged residues (E, pK_a of 4.05) at neutral pH (Scheme 1).[37] Thus, it is expected that the charge status of this peptide can be tuned by adjusting the solution pH. In an acidic environment, the peptide becomes positively charged, whereas it becomes negatively charged under basic conditions. A change in the peptide charge can affect its affinity to the negatively charged mica surface and the self-assembly behavior. Figure 3a−d shows AFM images of the assembled nanostructure formed after injecting a 100 μL of EAK16-II stock solution into 500 μL of 1 mM HCl, to yield a final peptide concentration of 2 μM and a solution pH value of 3.4. Only 2 min after the injection, many short nanofibers ranging in length from ~30 to 100 nm are observed on the mica substrate (Figure 3a). A slight increase in the nanofiber length is observed over time. After 17 min, the lengths range from ~110 to 490 nm (Figure 3d). A representative analysis of the variation of nanofiber length with time is plotted in Figure 3e. The nanofiber length increases linearly with time at a rate of 0.078 nm/s, which is ~7 times slower than that observed in pure water (Figure 1f). The pH (3.4) of this solution is lower than the pK_a of the glutamic acid and results in the partial neutralization of the glutamic acid residues and leads to a net positive charge of the peptide molecule. Repulsive forces between positively charged molecules may explain the observed decrease in the fiber growth rate. On the other hand, the more positively charged peptide nanofibers and molecules should more easily adhere to the negatively charged mica substrate, resulting in a significant increase in the amount of adsorbed EAK16-II nanofibers on mica at the start of the incubation time (compare Figure 1a with Figure 3a).

The assembly of EAK16-II in 10 mM HCl on mica was also investigated. Figure 4, panels a and b, shows the in situ AFM images of EAK16-II nanofibers on the mica surface in this solution having a measured pH of 2.2. Within about 2 min after

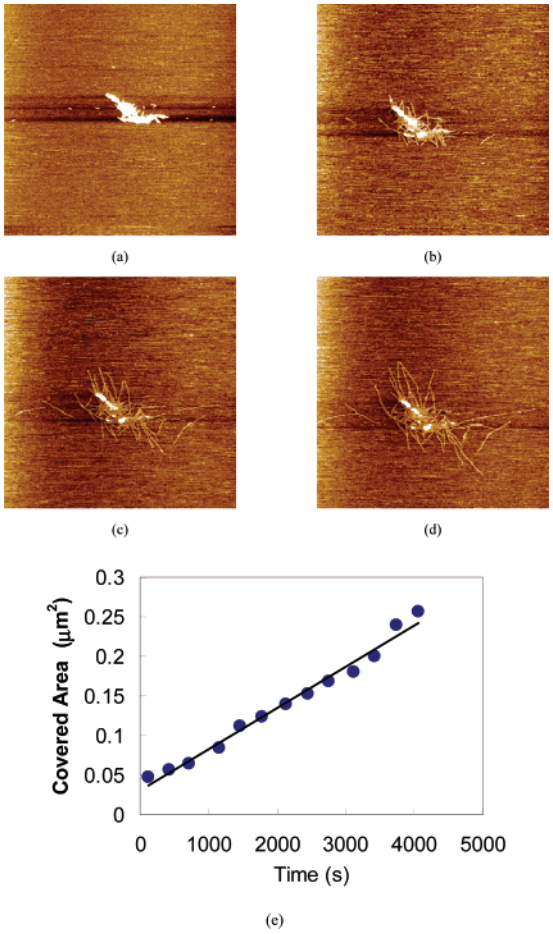

Figure 2. Time evolution of EAK16-II nanofiber growth from fiber clusters in pure water at (a) 120, (b) 1320, (c) 2520, and (d) 3120 s. The area covered by the clusters as a function of time is plotted in (e). Each in situ AFM image corresponds to a scan area of 2000 nm × 2000 nm.

(34) Scheibel, T.; Parthasarathy, R.; Sawicki, G.; Lin, X.-M.; Jaeger, H.; Lindquist, S. L. *Proc. Natl. Acad. Sci. U.S.A.* **2003**, *100*, 4527−4532.
(35) Nayak, R. R.; Roy, S.; Dey, J. *Polymer* **2005**, *46*, 12401−12409.
(36) Zhao, X.; Dai, J.; Zhang, S. *Mater. Res. Soc. Symp. Proc.* **2004**, *820*, O1.1.1−O1.1.11.
(37) Voet, D.; Voet, J. G.; Pratt, C. W. *Fundamentals of Biochemistry*, 2nd ed.; John Wiley & Sons, Inc: 2006.

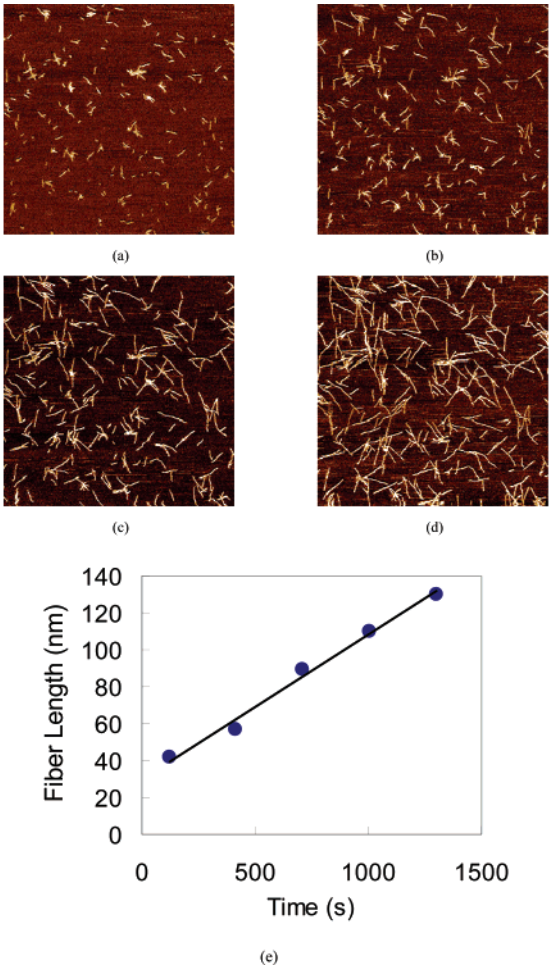

Figure 3. EAK16-II nanofiber growth on mica substrate in 1 mM HCl solution at (a) 120, (b) 420, (c) 720, and (d) 1020 s. The EAK16-II nanofiber length on mica in 1 mM HCl solution is plotted as a function of time in panel (e). Each in situ AFM image corresponds to a scan area of 2000 nm × 2000 nm.

the addition of the peptide solution to the HCl solution, short nanofibers are observed to densely cover the surface (Figure 4a). After ~19 min, no significant change in fiber length is observed (Figure 4b), indicating that very little growth of these fibers occurs in such a solution. The very acidic environment could make the EAK16-II molecules positively charged enough to inhibit peptide−peptide and peptide−nanofiber assembly. On the other hand, this would tend to strengthen the affinity of the nanofibers to the negative mica surface relative to that observed in pure water and 1 mM HCl solution and lead to a significant increase in the amount of EAK16-II adsorbed as nanofiber "seeds" on the surface (compare Figure 3a and Figure 4a).

The fact that very little growth of the nanofibers occurs after adsorption under highly acidic conditions may provide a method to characterize the dimensions of the nanofibers formed in the bulk solution. The nanofibers are stable upon injection into 10 mM HCl solution (see section 3.3). Therefore, the size of nanofibers in Figure 4, panels a and b, should reflect that of the nanofibers dissolved in the peptide stock solution. Figure 4c shows the length distribution of nanofibers shown in Figure 4a. The nanofibers in the peptide stock solution (12 μM) predominantly have lengths ranging from ~30 to 60 nm (average length of 54.6 ± 19.5 nm).

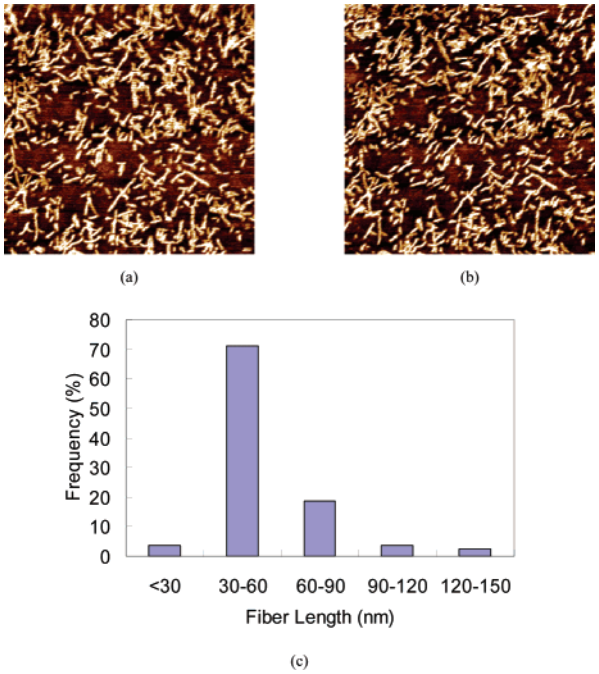

Figure 4. EAK16-II nanofiber growth on mica in 10 mM HCl solution at (a) 120 and (b) 1140 s. The fiber length distribution of EAK16-II in 10 mM HCl is plotted in panel (c). Each in situ AFM image corresponds to a scan area of 1000 nm × 1000 nm.

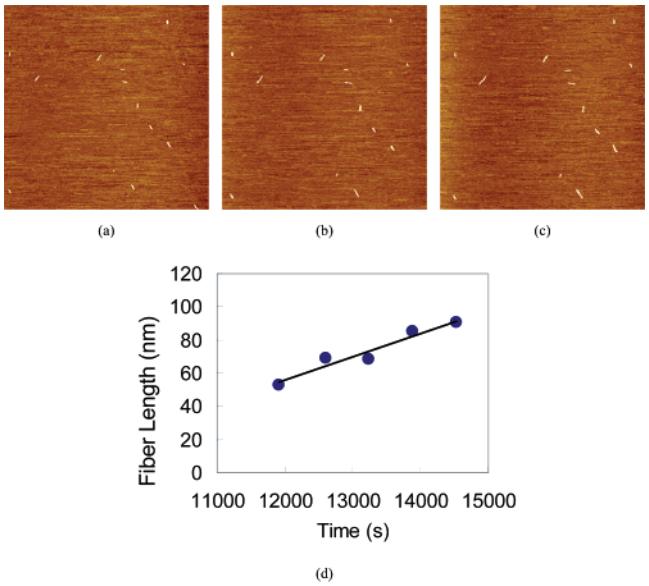

Figure 5. EAK16-II nanofiber growth on mica in 1 mM NaOH solution at (a) 11 820, (b) 12 420, and (c) 13 020 s. The EAK16-II fiber length on mica in 1 mM NaOH solution is plotted as a function of time in panel (d). Each in situ AFM image corresponds to a scan area of 2000 nm × 2000 nm.

EAK16-II molecules can become negatively charged when the solution pH is greater than the pK_a (10.54) of the lysine residues. Figure 5a−c shows the in situ AFM images of EAK16-II nanofibers growing on the mica substrate in 1 mM NaOH (final pH 9.9). Several short nanofibers with lengths ranging from ~20 to 55 nm are dispersed on the mica surface after 197 min incubation. The length of these fibers increases slightly with time (Figure 5, panels b and c). A representative plot of the fiber length as a function of time is shown in Figure 5d. The fiber length again increases linearly with time, similar to that

Figure 6. EAK16-II nanofiber growth on mica in 10 mM NaOH solution at (a) 5400 and (b) 6660 s. Each in situ AFM image corresponds to a scan area of 2000 nm × 2000 nm.

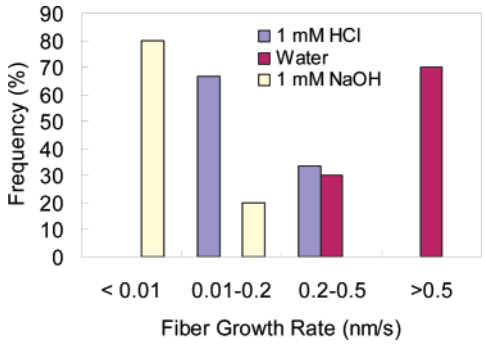

Figure 7. Histogram of EAK16-II nanofiber growth rates in pure water, 1 mM HCl, and 1 mM NaOH solutions.

observed in the other solutions. However, the growth rate is only 0.014 nm/s, much smaller than that in pure water and 1 mM HCl. When the NaOH concentration is further increased to 10 mM (pH 11.5 after the injection of peptide stock solution), no nanofibers are observed on the mica substrate in the first hour of incubation; after 1.5 h incubation, only a few fibers are observed (Figure 6). These nanofiber "seeds" do not grow during the experimental period.

A statistical analysis was conducted to obtain the distribution of EAK16-II nanofiber growth rates under the different solution conditions. The frequencies of the fiber growth rates within the following ranges are assigned to generate the histogram shown in Figure 7: very slow (<0.01 nm/s), slow (0.01−0.2 nm/s), intermediate (0.2−0.5 nm/s) and fast growth (>0.5 nm/s). In pure water solution, most nanofibers grow at a fast growth rate above 0.5 nm/s, whereas the peptide nanofibers grow predominantly at a slow speed of 0.01−0.2 nm/s in 1 mM HCl and even more slowly (<0.01 nm/s) in 1 mM NaOH solution. The average growth rates of the peptide nanofibers in the different environments are summarized in Table 1.

3.3. Self-Assembly of EAK16-II in Bulk Solution. 3.3.1. Dynamic Light Scattering of EAK16-II in Solution. To better analyze and understand the assembly behavior of EAK16-II on mica, the self-assembly process of EAK16-II in the bulk solutions was monitored using DLS. Figure 8a shows the time evolution of the scattered light intensity of 0.3 mM EAK16-II in pure water, 1 mM HCl, 10 mM HCl, and 10 mM NaOH solutions. For the peptide dissolved in pure water, the scattered light intensity rapidly increases with time at the outset before leveling off and slowly approaching a plateau after ~300 h (12.5 days), indicating that the self-assembly of the peptide has reached steady state. However, such an equilibrium state in peptide assembly will be changed when the peptide is in contact with the mica surface. Upon the adsorption on the surface, the active ends of the nanofiber "seeds" and fiber clusters can

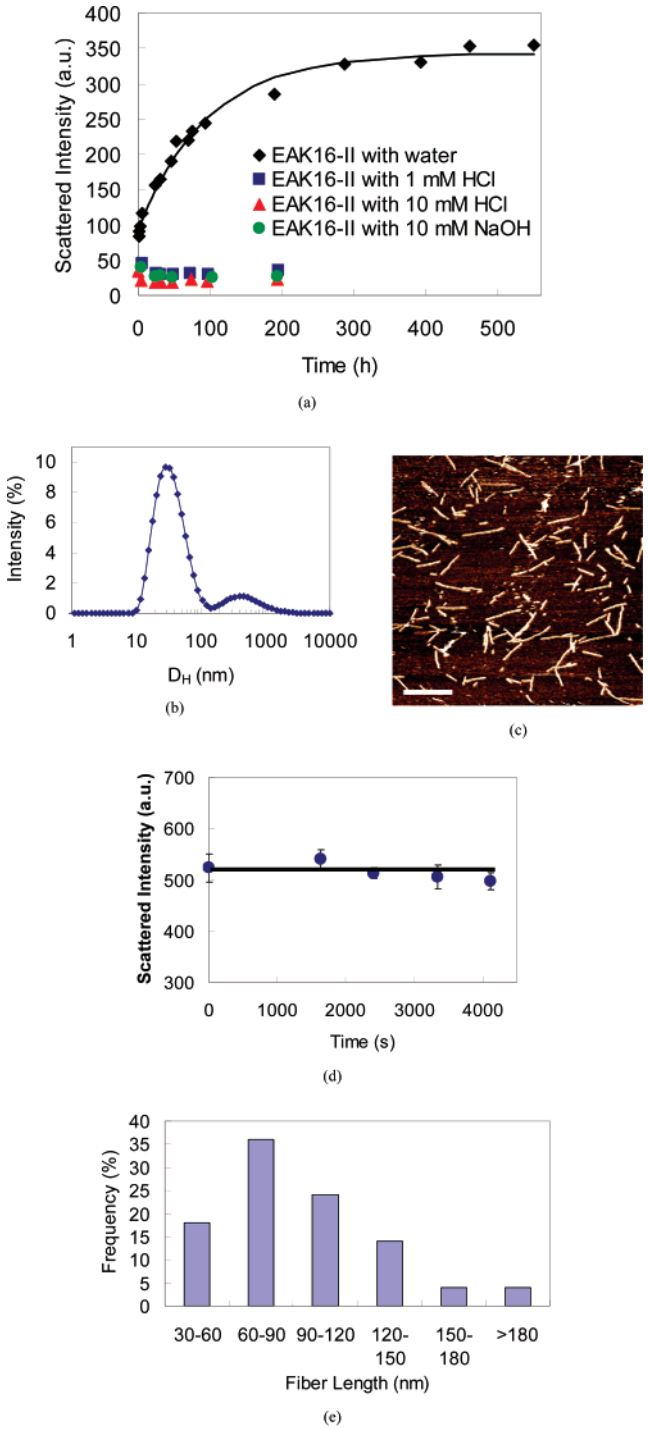

Figure 8. (a) Variation of scattering intensity of 0.3 mM EAK16-II in various aqueous solutions with time. The solid line represents a fitting curve to the eq 1. (b) Representative size distribution (based on the scattered intensity) of EAK16-II obtained in pure water after 55 h. (c) AFM image of 0.3 mM EAK16-II (prepared in pure water) after 550 h, obtained in 10 mM HCl solution. (d) Light intensity of EAK16-II aggregates in 10 mM HCl as a function of time. (e) The fiber length distribution obtained from AFM image in (c). Scale bar represents 200 nm.

continue to grow. The dramatic change of EAK16-II assembly due to the presence of a surface indicates that the nanofiber growth on mica is indeed a surface-assisted phenomenon.

On the other hand, the scattered light intensity shows no significant change with time in the case of the peptide dissolved in 1 mM HCl, 10 mM HCl, and 10 mM NaOH solutions. This

suggests that the peptide does not tend to self-assemble in these acidic and basic solutions. It has been reported that very acidic conditions can significantly slow the kinetics of the assembly of an amyloid peptide.[38] This may be due to the charge repulsion among peptide molecules under these solution conditions.

Figure 8b shows a representative hydrodynamic diameter distribution based on the light intensity of the peptide in pure water after 55 h of incubation. This shows two distinct size populations, one centered at ~33 nm and the other at 320 nm. The first population may correspond to the peptide nanofibers, whereas the second one may be associated with the fiber clusters. The presence of these two size populations in solution is consistent with the in situ AFM observation (Figures 1 and 2) of the coexistence of nanofibers and large fiber aggregates.

To compare the dimensions of the nanofibers observed by AFM with those obtained by DLS, AFM images of the aged peptide (0.3 mM EAK16-II in pure water after 550 h, having reached equilibrium state) were taken in 10 mM HCl (Figure 8c). The nanofibers observed on mica are taken to be those that originally formed in pure water for the following reasons. As shown above, EAK16-II nanofibers do not further grow on the mica substrate under very acidic solution conditions (e.g., Figure 4). Also, nanofibers formed in pure water have been found to remain stable for at least 1 h after their addition to a 10 mM HCl solution, as indicated in Figure 8d which shows very little change in the scattered light intensity of this solution over this period. This assures a new method using AFM to characterize the peptide assemblies in bulk solution, in addition to the well-known cryo-TEM technique, i.e., AFM imaging of peptide assemblies in an acidic solution.[39−41]

Images of 50 individual nanofibers obtained by AFM were analyzed to generate a distribution of their lengths (Figure 8e). This analysis shows that all nanofibers have lengths greater than 30 nm and the highest frequency is observed for lengths between 60 and 90 nm. The average nanofiber length is calculated to be 93.4 ± 37.8 nm. On the basis of the assumption that the nanofibers have a cylindrical shape, their length can be converted to a hydrodynamic diameter using the following equation:[38]

$$D_h = L\left(\sqrt{1-x^2}/\ln\frac{1+\sqrt{1-x^2}}{x}\right) \qquad (3)$$

where $x = d/L[1 + 0.37(L - d)/L]$, L is the fiber length, and d is the fiber width. The use of this equation yields a hydrodynamic diameter of 31 ± 8 nm ($n = 50$), which is very close to that obtained from the DLS experiment in water (~33 nm, Figure 8b). It should be noted that this estimation is approximate since the assumption that the nanofiber has a cylindrical shape may not be entirely correct. In fact, the EAK16-II nanofibers are ribbon-like, with their heights (~1−2 nm) being much smaller than their widths (~7 nm). In addition, these ribbon-like nanofibers may not be as rigid as a cylinder. However, no simple equation is available to correlate the hydrodynamic diameter with such a structure. Usually, a more complicated approach or analysis is required for fiber-like structures.[42,43] Regardless, this rough estimation shows a reasonable correlation between the AFM observation and the DLS measurement.

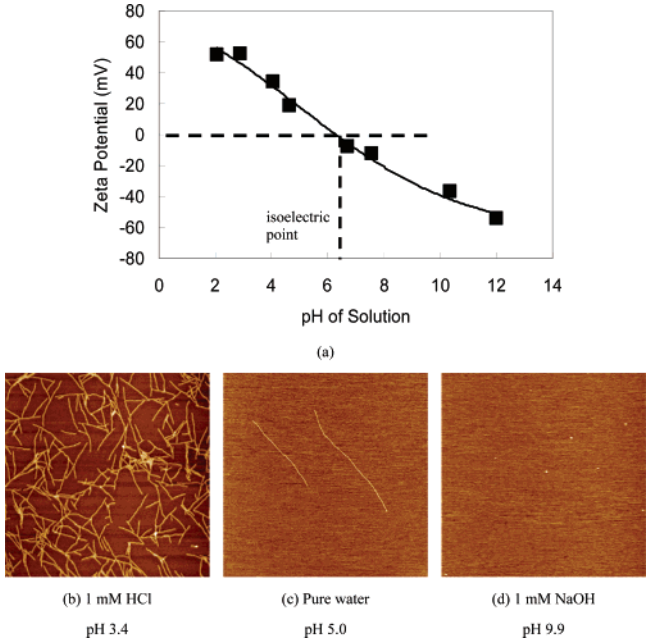

Figure 9. (a) ζ-Potential of EAK16-II as a function of pH. The standard deviation of ζ-potentials are less than 4 mV. (b−d) AFM images of EAK16-II on mica in various solutions after 30 min. Scan area is 2000 nm × 2000 nm.

3.3.2. ζ-Potential of EAK16-II. ζ-Potential measurements were made to determine the surface charge of EAK16-II assemblies in solution. The net surface charge of particles is an important parameter to predict their tendency to aggregate and adsorb onto surfaces. Theoretically, the larger the ζ-potential, either positive or negative, of a particle, the more stable the resulting suspension will tend to be (i.e., no aggregation). Figure 9a shows ζ-potentials of 0.18 mM EAK16-II solution as a function of solution pH. From this analysis, an isoelectric point (pI) for the EAK16-II system is found to be 6.3, which is comparable to the calculated pI value of 6.7 for the EAK16-II molecule.[22] Note that the pI being measured in these experiments is not for EAK16-II monomers alone but, rather, for a mixture of monomers and aggregates that exist in these EAK16-II solutions. Figure 9, panels b−d, shows the AFM images of 2 μM EAK16-II obtained in 1 mM HCl (final pH 3.4), pure water (final pH 5.0), and 1 mM NaOH (final pH 9.9) after 30 min of incubation. Densely dispersed and shorter nanofibers are observed at lower pH (1 mM HCl), whereas sparsely dispersed and longer nanofibers are observed at pH 5.0 close to the pI of the EAK16-II system. At pH 9.9, which is above the pI, no fibers are observed over the first 30 min.

When the ζ-potential results are compared with the AFM observations, it can be clearly seen that the charge status of the EAK16-II system is crucial to the assembly of EAK16-II on mica. At low pH, the peptides/nanofibers are positively charged

(38) Lomakin, A.; Chung, D. S.; Benedek, G. B.; Kirschner, D. A.; Teplow, D. B. *Proc. Natl. Acad. Sci. U.S.A.* **1996**, *93*, 1125−1129.
(39) Santoso, S.; Hwang, W.; Hartman, H.; Zhang, S. *Nano Lett.* **2002**, *2*, 687−691.
(40) Marini, D. M.; Hwang, W.; Lauffenburger, D. A.; Zhang, S.; Kamm, R. D. *Nano Lett.* **2002**, *2*, 295−299.
(41) Bonini, M.; Rossi, S.; Karlsson, G.; Almgren, M.; Lo Naostro, P.; Baglioni, P. *Langmuir* **2006**, *22*, 1478−1484.
(42) Aggeli, A.; Fytas, G.; Vlassopoulos, D.; McLeish, T. C. B.; Mawer, P. J.; Boden, N. *Biomacromolecules* **2001**, *2*, 378−388.
(43) Georgalis, Y.; Starikov, E. B.; Hollenbach, B.; Lurz, R.; Scherzinger, E.; Saenger, W.; Lehrach, H.; Wanker, E. E. *Proc. Natl. Acad. Sci. U.S.A.* **1998**, *95*, 6118−6121.

(very positive ζ-potential) and so have a strong affinity for the negatively charged mica surface, leading to a dense dispersion on the surface (Figure 9b). However, the electrostatic repulsion between peptides tends to retard fiber growth (Figures 3 and 4, Table 1) and yield shorter lengths. In pure water, on the other hand, the attraction between the peptide and the mica surface is moderate, but less repulsion between peptide molecules/fibers results due to a close to zero ζ-potential. Thus, on the same time scale, fewer but longer peptide nanofibers than in 1 mM HCl are observed on mica (Figure 9c). The absence of nanofibers in 1 mM NaOH (Figure 9d) is likely due to the large electrostatic repulsion between the negatively charged peptide and the mica surface. Under this condition, nanofibers appear only after a long incubation time (197 min) and the fiber growth rate is very low (Figure 5 and Table 1)

4. Discussion

4.1. Control of Nanofiber Growth on Mica by Adjusting Solution pH. Surface-assisted assembly of EAK16-II on mica appears to be governed by two principal interactions: (1) peptide−surface interaction that enables nanofiber "seeds" and fiber clusters to adsorb onto mica and serve as "nuclei"; (2) peptide−peptide interaction that enables elongation of the nanofiber "nuclei". A simple way to control this process is to modulate the two interactions by adjusting the solution pH.

4.1.1. Peptide−Surface Interaction. At different pHs, the amount of nanofibers deposited on the mica surface at the same time scale can be significantly altered and follows the order 10 mM HCl > 1 mM HCl > pure water > 1 mM NaOH > 10 mM NaOH. This is because the charge status of the peptide monomers and aggregates can be changed according to different solution pHs. By adjusting the solution pH, one could control the adsorption of the nanofiber "seeds" to mica, which will determine the density of growing nanofibers on the surface.

The adsorption of the nanofiber "seeds" on a surface is a prerequisite for surface-assisted nanofiber growth. The deposited nanofiber "seeds" serve as the nuclei for subsequent fiber growth. A high affinity for a surface will concentrate peptides at the surface and facilitate peptide−peptide association. This also explains why nanofiber growth of EAK16-II on mica is possible at a peptide concentration of 2 μM, much lower than its critical aggregation concentration (CAC) of ∼60 μM.[21] The importance of the surface charge on the adsorption of peptides and proteins onto surfaces of mica and micelles has been demonstrated by Zhu et al.[16] and Necula et al.[44] It is also worth noting that the surface restricts the mobility of the adsorbed nanofibers and may influence their growth mode.

4.1.2. Peptide−Peptide Interaction. Although the peptide−surface interaction initiates surface-assisted assembly, the growth of deposited nanofiber "seeds" is mainly controlled by peptide−peptide interaction. The growth rate of EAK16-II nanofibers on mica in various solutions follows the order pure water > 1 mM HCl > 1 mM NaOH > 10 mM HCl ≈ 10 mM NaOH ≈ 0 (Table 1 and Figure 7). This is because the peptide−peptide association can be significantly affected by the electrostatic repulsion. The fastest nanofiber growth occurs in pure water, where the electrostatic repulsion is minimum. The electrostatic repulsion increases in acidic or basic solutions, which resists the peptide−peptide association, leading to slower or none fiber growth. By adjusting the solution pH, one could control the growth of the nanofiber "seeds", which further determines the length of the growing nanofibers at a given time period.

Scheme 2. Proposed Model of EAK16-II Nanofiber Growth on Mica

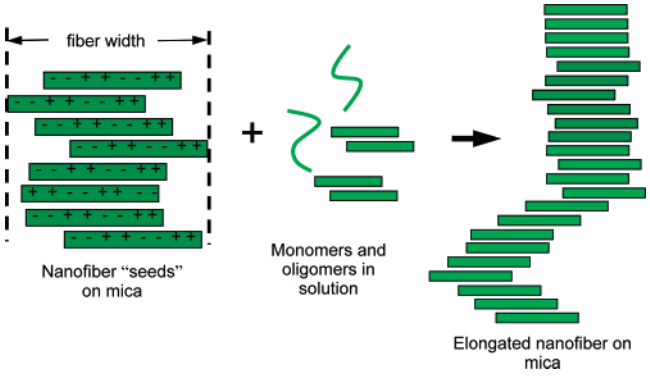

Overall, the surface-assisted nanofiber growth of EAK16-II can be controlled by adjusting the solution pH to have the desired amount and dimension (long or short) of the nanofibers. The amount of nanofibers deposited on the surface can be regulated at the step of "nucleation" (i.e., the adsorption of the nanofiber "seeds" to mica); the strength of the electrostatic repulsion between peptide molecules will determine the growth rate of the nanofibers and further control the length of nanofibers at a specific time. The controllable nanofiber growth on a surface may be beneficial to fabricate many peptide-based functional nanostructures.

4.2. Proposed Model of EAK16-II Nanofiber Growth on Mica. All AFM images have shown that the nanofibers formed on mica have a uniform width of ∼7 nm and a height ranging from ∼1 to 2 nm. Our previous results have shown that EAK16-II predominantly adopts a β-sheet secondary structure in aqueous solution.[20] The height of a single β-sheet of EAK16-II can be estimated to be ∼1 nm. Comparison of this value with the observed nanofiber height of EAK16-II (∼1−2 nm) suggests that the EAK16-II nanofibers observed on mica are probably made of one or two β-sheet layers. The width of nanofibers of ∼7 nm from the AFM results is very close to the length of an EAK16-II molecule in β-strand conformation (∼5.9 nm). Thus, we may propose that EAK16-II adopts a cross-β-sheet arrangement when forming nanofibers (i.e., the peptide β-strands are arranged perpendicularly to the direction of fiber elongation).

Accordingly, a simple model of EAK16-II nanofiber growth on the mica surface may be proposed in Scheme 2. EAK16-II nanofiber "seeds" first adsorb on mica. These nanofibers are probably made of single or double layers of β-sheets. The two active ends of the nanofiber can further associate with peptide monomers or oligomers and continue to grow. Peptide−peptide interactions may involve hydrogen bonding between backbones, electrostatic attraction between charged residues, and hydrophobic interaction between A residues. When a peptide monomer interacts with a β-strand at one active end, the electrostatic interaction, due to the ionic complementarity, may allow it to shift in the direction perpendicular to the fiber length, as shown in Scheme 2. This may explain why nanofibers are sometimes observed to have a wavy shape along its length. This model may also explain why the nanofibers have a consistent width. However, whether these β-sheets preferentially adopt an anti-

(44) Necula, M.; Chirita, C. N.; Kuret, J. *J. Biol. Chem.* **2003**, *278*, 46674−46680.

parallel or parallel fashion is still unclear since both arrangements can occur in an ionic-complementary peptide. Further experiments, such as solid-state NMR and X-ray fiber diffraction, are required to distinguish these two arrangements.

4.3. Significance of Surface-Assisted Peptide Assembly. 4.3.1. Comparison of EAK16-II Assembly with Amyloid Fibrillization. The surface-assisted assembly of EAK16-II has many similarities to amyloid fibrillization, which is a main characteristic of many conformational diseases.[45,46] Surface-assisted EAK16-II nanofiber growth seems to follow a nucleation and growth mechanism. The deposited nanofiber seeds or fiber clusters can serve as nuclei on the hydrophilic, negatively charged mica surface for surface-assisted nanofiber growth. This mechanism is similar to that of protein/peptide fibrillogenesis in bulk solution.[38,47−54] The growth of the deposited nanofiber "seeds" is bidirectional (i.e., from two active ends); such a growth pattern has been found in the fibrillization of synthetic human amylin,[55] β-amyloid,[18] and prion protein either in solution or on a surface.[56,57] The nanofiber growth from the fiber clusters is radial and unidirectional, which is also similar to amyloid fibrillization on mica and glass substrates.[15,16,18] The kinetics of EAK16-II assembly is significantly increased upon adsorption on a negatively charged mica surface at a very low peptide concentration (2 μM). This is much the same as the finding that anionic micelles can greatly accelerate fibrillization of recombinant α-synuclein at low micromolar concentrations.[44] These similar characteristics between EAK16-II and disease-related peptides/proteins suggest that a simple model peptide may be used to study the surface effect of the more complicated amyloid fibrillization.

This study has demonstrated that the assembly of EAK16-II on the negatively charged mica surface can be controlled by modulating the peptide surface charges. The repulsion between negatively charge peptides and mica inhibits their adsorption and growth. This may provide a means to control amyloid fibrillization on negatively charged cell membranes. It has been found that the binding of amyloid-β peptides to cell membranes facilitates amyloid fibrillization, which in turn disturbs the structure and function of the membranes (e.g., membrane fluidity and ion channels).[58,59] If the amyloid peptides/proteins becomes very negatively charged, their ability to bind to the cell membrane and surface-induced fibrillization may be significantly reduced. This could be achieved by introducing negatively charged molecules (e.g., polyglutamates) grafted with a binding motif to these amyloid peptides/proteins.

4.3.2. Potential Application in Biomolecular Sensing. Understanding and controlling the surface-assisted peptide assembly is beneficial to construct many biocompatible devices, such as immunosensors[60] and enzyme biosensors.[61] Such devices often require surface modification to immobilize biomolecules on various conducting matrices. The surface modifying materials should contain reactive groups to immobilize biomolecules, enhance the stability and maintain the activity of the immobilized proteins/enzymes, as well as reduce the blockage of electron transfer from the proteins/enzymes to the electrode (for amperometric sensors). Self-assembling peptides could be one ideal material for these purposes. We have utilized EAK16-II assembled nanostructures to modify an electron conductive highly ordered pyrolytic graphite (HOPG) electrode. An amperometric enzyme biosensor was successfully fabricated using this EAK16-II modified electrode by immobilizing a model enzyme of glucose oxidase (GOx) to the carboxylate groups on EAK16-II. The immobilized GOx exhibits good catalytic activity upon the addition of glucose. Further detailed studies of peptide modified electrodes as biosensors will be reported in the near future.

5. Conclusions

The growth of EAK16-II nanofibers on a mica surface has been observed via in situ AFM. The growth kinetics of single nanofibers can be directly quantified. In pure water, the average nanofiber growth rate is 0.74 ± 0.40 nm/s. The nanofiber growth appears to follow a nucleation and growth mechanism that involves the adsorption of nanofiber "seeds" or fiber clusters formed in stock solution, to serve as nuclei, and fiber elongation at the active ends of these nuclei. Dynamic light scattering experiments indicate that the nanofiber growth is a surface-assisted phenomenon; nanofibers that no longer grow in solution can start to grow once they adsorb onto the surface. Such surface-assisted nanofiber growth can be controlled by adjusting the solution pH to regulate both nucleation and growth steps. The amount of nanofiber "seeds" that adsorb on mica decreases as the solution pH increases. The growth rate of EAK16-II nanofibers in different solutions follows the order pure water $>$ 1 mM HCl $>$ 1 mM NaOH $>$ 10 mM HCl $\approx$ 10 mM NaOH $\approx$ 0. This controllable nanofiber growth may be beneficial to the construction of functional, supramolecular structures. We have demonstrated that, at very acidic condition (10 mM HCl), in situ AFM is capable of directly "seeing" the assemblies formed in the bulk solution. The surface-assisted EAK16-II assembly has many similar characteristics to amyloid fibrillization on surfaces. This study provides a model to help understand and control surface-assisted fibrillization of disease-related peptides/proteins. The controllable peptide assembly on the surface has an exciting potential application in constructing biocompatible electrodes for biosensors.

Acknowledgment. We thank Dr. Yooseong Hong and Professor G. A. Scholz for help with the TEM experiment. We

(45) Stefani, M.; Dobson, C. M. *J. Mol. Med.* **2003**, *81*, 678−699.
(46) Murphy, R. M. *Annu. Rev. Biomed. Eng.* **2002**, *4*, 155−174.
(47) Walsh, D. M.; Hartley, D. M.; Kusumoto, Y.; Fezoui, Y.; Condron, M. M.; Lomakin, A.; Benedek, G. B.; Selkoe, D. J.; Teplow, D. B. *J. Biol. Chem.* **1999**, *274*, 25945−25952.
(48) Wood, S. J.; Wypych, J.; Steavenson, S.; Louis, J.-C.; Citron, M.; Biere, A. L. *J. Biol. Chem.* **1999**, *274*, 19509−19512.
(49) Scherzinger, E.; Sittler, A.; Schweiger, K.; Heiser, V.; Lurz, R.; Hasenbank, R.; Bates, G. P.; Lehrach, H.; Wanker, E. E. *Proc. Natl. Acad. Sci. U.S.A.* **1999**, *96*, 4604−4609.
(50) Kayed, R.; Bernhagen, J.; Greenfield, N.; Sweimeh, K.; Brunner, H.; Voelter, W.; Kapurniotu, A. *J. Mol. Biol.* **1999**, *287*, 781−796.
(51) Friedhoff, P.; von Bergen, M.; Mandelkow, E.-M.; Davies, P.; Mandelkow, E. *Proc. Natl. Acad. Sci. U.S.A.* **1998**, *95*, 15712−15717.
(52) Rhoades, E.; Agarwal, J.; Gafni, A. *Biochim. Biophys. Acta* **2000**, *1476*, 230−238.
(53) Kim, Y.-S.; Randolph, T. W.; Stevens, F. J.; Carpenter, J. F. *J. Biol. Chem.* **2002**, *277*, 27240−27246.
(54) Librizzi, F.; Rischel, C. *Protein Sci.* **2005**, *14*, 3129−3134.
(55) Goldsbury, C.; Kistler, J.; Aebi, U.; Arvinte, T.; Cooper, G. J. S. *J. Mol. Biol.* **1999**, *285*, 33−39.
(56) Depace, A. H.; Weissman, J. S. *Nat. Struct. Biol.* **2002**, *9*, 389−396.
(57) Scheibel, T.; Kowal, A. S.; Bloom, J. D.; Lindquist, S. L. *Curr. Biol.* **2001**, *11*, 366−369.
(58) Verdier, Y.; Zarandi, M.; Penke, B. *J. Pept. Sci.* **2004**, *10*, 229−248.
(59) Yip, C. M.; McLaurin, J. *Biophys. J.* **2001**, *80*, 1359−1371.
(60) Adanyi, N.; Varadi, M.; Kim, N.; Szendro, I. *Curr. Appl. Phys.* **2006**, *6*, 279−286.
(61) Mena, M. L.; Carralero, V.; Gonzalez-Cortes, A.; Yanez-Sedeno, P.; Pingarron, J. M. *Electroanalysis* **2005**, *17*, 2155.

also acknowledge Professor Elizabeth Meiering for allowing use of the instrument to conduct DLS and ζ-potential experiments. We thank Jason Dockendorff for help with viscosity measurement. We thank Yuebiao Sheng for helpful discussion. Support for this research has been provided by the Natural Sciences and Engineering Research Council of Canada (NSERC), Canadian Foundation for Innovation (CFI), and the Canada Research Chairs (CRC) Program for one of the coauthors (P.C.).

JA073168U